

Objective Amplitude of Accommodation Computed from Optical Quality Metrics Applied to Wavefront Outcomes

Norberto López-Gil¹, Vicente Fernández-Sánchez¹, Larry N. Thibos² and Robert Montés-Micó³

ABSTRACT

PURPOSE: We studied the accuracy and precision of 32 objective wavefront methods for finding the amplitude of accommodation obtained in 180 eyes.

METHODS: Ocular accommodation was stimulated with 0.5 D steps in target vergence spanning the full range of accommodation for each subject. Subjective monocular amplitude of accommodation was measured using two clinical methods, using negative lenses and with a custom Badal optometer.

RESULTS: Both subjective methods gave similar results. Results obtained from the Badal optometer were used to test the accuracy of the objective methods. All objective methods showed lower amplitude of accommodation than the subjective ones by an amount that varied from 0.2 to 1.1 D depending on the method. The precision in this prediction also varied between subjects, with an average standard error of the mean of 0.1 D that decreased with age.

CONCLUSIONS: Depth of field increases subjective of amplitude of accommodation overestimating the objective amplitude obtained with all the metrics used. The change in the negative direction of spherical aberration during accommodation increases the amplitude of accommodation by an amount that varies with age.

(J Optom 2009;2:223-234 ©2009 Spanish Council of Optometry)

KEY WORDS: image quality metrics; amplitude of accommodation; presbyopia; subjective methods; objective methods.

RESUMEN

OBJETIVO: Estudiamos la exactitud y la precisión de 32 métodos objetivos de calidad de imagen aplicados al frente de onda ocular y utilizados para calcular la amplitud de acomodación en 180 ojos.

MÉTODOS: Se estimuló la acomodación ocular modificando la vergencia del estímulo a pasos de 0,5 D, de forma que se cubriese todo el rango de acomodación de cada sujeto. Se midió la amplitud de acomodación monocular subjetiva utilizando dos métodos habituales en la práctica clínica: uno basado en el uso de lentes negativas y otro basado en un optómetro de Badal adaptado.

RESULTADOS: Con ambos métodos subjetivos se obtuvieron resultados parecidos. Los resultados obtenidos con el método basado en

el optómetro de Badal se utilizaron para evaluar la exactitud de los métodos objetivos. En todos los casos, con todos los métodos objetivos se obtuvo una menor amplitud de acomodación que con los subjetivos; la diferencia entre ambos tipos osciló entre 0,2 D y 1,1 D, dependiendo de cada sujeto concreto. La precisión de esta estimación también varió entre un sujeto y otro: el error estándar de la media fue, en promedio, igual a 0,1 D, disminuyendo con la edad. **CONCLUSIONES:** La profundidad de campo aumenta la amplitud de acomodación subjetiva que sobrestima los valores objetivos encontrados por cualquiera de los métodos objetivos usados. Los resultados indican que la variación, hacia valores más negativos, de la aberración esférica durante el proceso de acomodación hace que aumente la amplitud de acomodación en una cantidad que varía con la edad. (J Optom 2009;2:223-234 ©2009 Consejo General de Colegios de Ópticos-Optometristas de España)

PALABRAS CLAVE: métricas de calidad de imagen; amplitud de acomodación; presbicia; métodos subjetivos; métodos objetivos.

INTRODUCTION

Accommodation in humans is achieved by a change in the dioptric power of the crystalline lens.¹ The accommodative system maintains the image plane close to the entrance apertures of the foveal cone photoreceptors, even as the distance of an object changes. For the most part, accommodation and its reduction with age have been measured classically using two subjective methods: the push-up² and the minus-lens³ techniques. Although a subjective test provides important information about near visual ability, it does not accurately measure the accommodative optical change that occurs in the eye. This is because the eye's depth-of-field causes subjective measurements to overestimate the objectively measured accommodative amplitude^{4,5} unencumbered by depth-of-field effects. For example, open-field-of-view autorefractors⁶⁻⁹ are commonly used to obtain accurate, objective measurements of accommodation.⁸⁻¹² One purpose of the present study was to develop a novel method based on wavefront technology.

Recently, largely due to the development of clinical wavefront aberrometers, we are able to apply wavefront technology to measure ocular aberrations when the eye accommodates.¹³⁻¹⁸ Wavefront aberrometers provide a detailed description of the eye's focusing power at every point in the eye's pupil. Converting these detailed measurements into a clinical prescription for the ideal spherocylindrical correction is a process called wavefront refraction.¹⁹ One approach to wavefront refraction is to fit the two-dimensional wavefront aberration function with a quadratic surface that represents the wavefront produced by the optimum spherocylindrical lens. The two most common ways to perform this

From ¹Instituto de Envejecimiento, University of Murcia, Murcia, Spain.

²School of Optometry, Indiana University, Indiana, USA. ³Grupo de Investigación en Optometría (GIO), University of Valencia, Spain

Acknowledgements: This work has been supported in part by several grants from the Fundación SENECA, Comunidad Autónoma de la Región de Murcia to Norberto López-Gil (#00702/PPC/041# and #0583/PI/07#) and from the Ministerio de Ciencia e Innovación Research Grants to Robert Montés-Micó (#SAF2008-01114# and #SAF2009-13342#). Development of wavefront refraction methodologies has been supported by a grant from the US National Institutes of Health (#R01-EY05109) to Larry Thibos.

Financial Disclosure: Thibos has a proprietary interest in the development of optical metrics predictive of visual performance.

Received: 1 August 2009

Revised: 2 November 2009

Accepted: 18 November 2009

Corresponding author: Norberto López-Gil, Edificio D, Universidad de Murcia, 30100 Murcia, Spain
e-mail: norberto@um.es

fit are least-squares fitting over the full pupil and paraxial-curvature matching at the pupil center. The least-squares method, also known as a Zernike refraction, takes account of the eye's higher-order aberrations when determining the best correcting lens. By comparison, the paraxial method, also known as Seidel refraction, takes into account only the lower-order aberrations responsible for the curvature of the wavefront at the pupil center. The eye's higher-order aberrations do not affect wavefront curvature and are thus ignored. Paradoxically, the formulas for the parameters of the spherocylindrical lens that optimally corrects the paraxial wavefront involve the higher-order Zernike coefficients; this is necessary to eliminate the impact of higher-order aberrations from the Zernike coefficients for defocus and astigmatism.

A second approach to wavefront refraction is analogous to the process of subjective refraction, in which the clinician finds the combination of spherical and cylindrical lenses that optimize the clarity of the retinal image. The objective version, analogous to this subjective process, is to use a computer to find the particular combination of spherical and cylindrical lenses that optimize a given metric of retinal image quality for an object located at infinity. The mean spherical equivalent of this lens combination is equal to the target vergence required to optimize image quality; thus, this spherical equivalent represents the eye's refractive error. From an optical perspective, we think of the spherical equivalent as the vergence of a plane that is optically conjugate to the retina. In clinical parlance, the spherical equivalent is simply "the refraction".

Since wavefront refraction determines the plane that is optically conjugate to the retina, it can be used more generally to determine the refractive state of an accommodating eye. Changes in the refractive state thus quantify the accommodative response to a change in accommodative stimulus. The aim of our study was to compare the amplitude of accommodation (AA) determined by means of this wavefront technique with the traditional, subjective methods used in clinical and visual science, and also in clinical practice.

METHODS

Subjects

The study included 180 eyes (88 right ones and 92 left ones) from 98 subjects. All of them were Spaniards and most of the younger ones (less than 24 years old) were students from Murcia's School of Optometry. Age ranged from 20 to 58, with a corresponding mean and standard deviation of 35.6 ± 12.3 and 35.0 ± 12.4 years for eyes and subjects, respectively. Subjects read and signed an informed consent form that had been previously approved by the Ethics Committee of the University of Murcia. They also approved the experiment itself, which followed the tenets of the Declaration of Helsinki.

Subjects who normally wear contact lenses removed their lenses at least 24 (hydrophilic contact lenses) or 48 hours (gas-permeable contact lenses) before the experiment. A preliminary optometric study was performed, which included autorefractometry by means of a Canon Tomey TL-1000®, retinoscopy, and subjective refraction by with trial lenses. The results of this preliminary test, together with a questionnaire, provided a basis for exclusion from the experiment. The

exclusion criteria were: amblyopia; any kind of accommodative anomaly; continuous pharmacological treatment that could modify the accommodative mechanism; any kind of ocular surgery (including refractive surgery); and any kind of ocular disease that could affect vision or the accommodative mechanism (such as glaucoma, conjunctivitis or cataracts). These criteria were applied after the subject's medical history. Accommodation anomalies in young subjects were detected when the accommodative amplitude measured using negative lenses (see next subsection) was always smaller than the minimum one suggested by the Hofstetter formula²² and the accommodative flexibility was smaller than 11 cycles per minute, under monocular conditions.

From the initial 99 subjects not excluded by these criteria, only one could not accommodate to the visual target used in our experiments, so the data from that subject were removed from the study.

Subjective Measurement of the Amplitude of Accommodation

The subjective measurement of the amplitude of accommodation was performed using a custom-made Badal Optometer which was integrated in the refraction unit. As accommodation stimulus, it used a Bailey-Lovie chart (luminance = 100 cd/m²) located 6 m (20 feet) away from the subject. The Badal optometer consisted of two well-aligned achromatic doublets (focal length = 100 mm) as described elsewhere.²¹ One of the lenses was located at a distance of 100 mm from the eye's entrance pupil. This distance was fixed for each subject using a focusing camera that displayed a clear image of the subject's iris when the correct distance was achieved. The second doublet was free to be moved axially during the experiment by the observer, by means of a joystick. The precision of the positioning of the lens was 1 mm, corresponding to 0.1 D of target vergence. The subject's head was fixed using a chin rest. The subject's astigmatism, if any, was corrected by means of a trial lens placed 1.2 cm in front of the eye. The possible refraction changes due to the astigmatism and the distance between the target and the moving achromatic lens was taken into account in the calculations.

The subject's task was to find the two extreme positions of the Badal optometer's mobile lens where the line containing 0.8 VA (20/25) letters was still clear without any perceptible blur. We refer to this dioptric range between near-point and far-point as the subjective AA. For comparison purposes, we also used a standard clinical method for determining the subjective AA, in which minus lenses are used to induce changes in vergence of a target located at a fixed viewing distance. As in the Badal method, astigmatism was corrected using trial lenses.

All the subjective measurements were performed by the same researcher, who was a trained optometrist. Distances between negative lenses and the eye were also taken into account in the calculations. The measurements were performed 3 times for the minus-lens method and 5 times for the Badal method (5 for the far point and another 5 for the near point). Mean and standard deviation of the measurements was similar for both methods, so we adopted the Badal

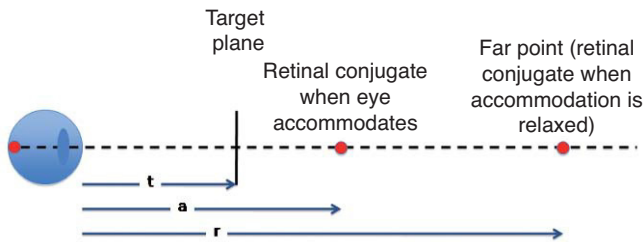


FIGURE 1
Definition of terms. Target vergence T is equal to the inverse of the viewing distance “ t ”. Distance “ r ” is equal to the axial position of the plane conjugate to the foveal cone apertures when accommodation is relaxed. The axial location of this retinal conjugate plane is called the “far point”. The refractive error of the eye equals the vergence ($1/r$) of the far point. The refractive state of the accommodated eye is defined as the vergence ($1/a$) of the retinal conjugate plane. Wavefront refraction is based on the assumption that the vergence of the retinal conjugate plane is the same as the target vergence required to maximize retinal image quality.

optometer technique as our preferred method because it was more precise due to its superior resolution (0.1 D, compared to 0.25 D for the minus-lens method). Moreover, the Badal-optometer experiment was quicker and simpler than the measurements done with the minus-lenses method.

Objective Measurement of the Amplitude of Accommodation

When a subject views a target intended to stimulate accommodation (see Figure 1), we anticipate that the eye’s refractive state will change in order to clearly focus the target onto the foveal cone apertures. To the extent that this does not happen, the eye exhibits an error of accommodation. Our goal was to measure the maximum change in the refractive state that could be achieved by manipulating target vergence. To quantify this outcome, we used the wavefront aberrometer to determine the eye’s refractive state, defined here as the target vergence required to maximize retinal image quality. This definition is based on the fundamental principle that to optimize retinal image quality, the target must be optically conjugate to the cone photoreceptor apertures. Thus, the vergence of the plane that is optically conjugate to the retina determines the eye’s refractive state. When accommodation is fully relaxed, the eye’s refractive state is also its refractive error, both of which are equal to the vergence of the far point (i.e. the retinal conjugate of the relaxed eye). These various distances and their corresponding vergences are summarized with reference to figure 1 as follows:

1. Target vergence: $T = 1/\text{target distance} = 1/t$
2. Refractive state of accommodated eye: $A = 1/a$
3. Refractive error of relaxed eye: $R = 1/r$

All distances are referred to the corneal plane and, according to the standard ophthalmic sign convention, they are negatives if the corresponding points are located in front of the eye, as in figure 1. Values for T , A , and R are equal to the power K of an ideal lens placed in the pupil plane that forms a virtual image at infinity of the target plane, the retinal conjugates when eye accommodates, or far point, respectively. Accommodation stimulus, AS , is defined as the change in target vergence: $AS = R - T$. Accommodation response, AR , is

defined as the change in refractive state of the accommodated eye compared to the relaxed eye: $AR = R - A$. Thus, to find the accommodation response we have to find the power of two ideal lenses, which correspond to the refraction, R , and to the refractive state of the accommodated eye, A . This is achieved by means of a through-focus calculation described next.

Since the power of the eye varies across the pupil area when higher-order aberrations are present, different conjugate foveal planes would be found depending on the pupil zone used and, therefore, the value of K would change across the pupil. The average K value that produces a “good image” for an ideal point object placed at the fovea and a natural pupil (assumed to have a circular shape), for a particular accommodation state, will depend on the particular definition of “good image” that we use. In this sense, we need to choose a metric that quantifies image quality and then we have to look for the target vergence that maximizes that metric. A variety of optical-quality metrics are available for this purpose, many of which were evaluated by Thibos et al.²² for predicting the refractive state of the relaxed eye. Some metrics quantify the quality of the eye’s wavefront aberration function, whereas others quantify the quality of the point spread function or of the optical transfer function associated with the retinal image. For a detailed mathematical description of these metrics see Appendix A in reference Thibos et al.²²

We have applied all 32 independent metrics described by Thibos et al.²² to determine the refractive state of the eye at various levels of accommodative response, including the relaxed eye. Appendix A shows a table with the names and some information of all the metrics used. The procedure followed for each subject consisted of two steps. In the first step, 3 wavefront aberration functions were obtained for the un-accommodated eye using the IRX3 aberrometer (Imagine Eyes, France). To ensure that the eye is unaccommodated, the aberrometer uses a fogging method in which the target distance is increased in 1 D steps while the eye’s refractive state is continuously monitored. When the eye fails to change its refractive state in the hyperopic direction in response to the change in target vergence, then accommodation is assumed to be fully relaxed. From three consecutive measurements taken over 10 s in this relaxed state, the more hyperopic one was selected as the reference to be used when computing the accommodative response. In this case, the refraction is obtained from the second-order Zernike coefficient C_2^0 obtained from a least-squares fit of a sphero-cylindrical surface to the wavefront. The wavefront corresponding to the unaccommodated eye is named $W_0(T_0)$.

In the second step, three repeated sets of wavefronts were recorded for the accommodated eye by using a stimulus vergence that changes automatically in steps of 0.5 D. After each movement of the target, there was a delay of 1.5 s before a wavefront measurement was made, in order to give the subject enough time to accommodate. From the refraction obtained in the first step, we added 0.5 D to the nearest hyperopic vergence multiple of 0.5 D (for instance, if the Zernike refractive error was 2.17 D, we obtained 2.5D + 0.5 D = 3 D; or if was -2.34 D we used -2 D + 0.5 D = -1.5 D). This value became the vergence of the first position of the stimulus in a series of accommodation measurements.

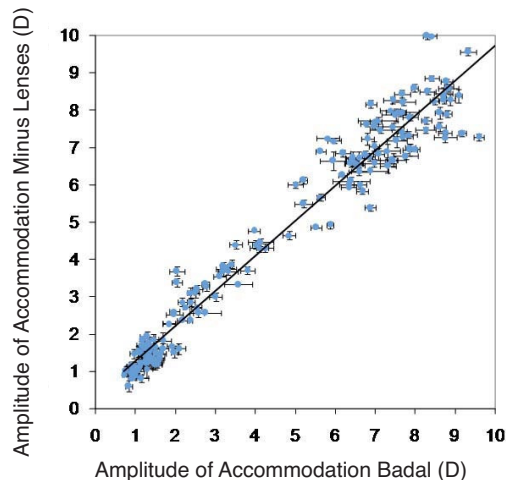


FIGURE 2 Subjective amplitude of accommodation measured with the minus-lenses and with the Badal methods. Error bars represent the intra-subject \pm SD. Least-square-fitted black line: $y=0.939x+0.3241$, $r^2=0.96$.

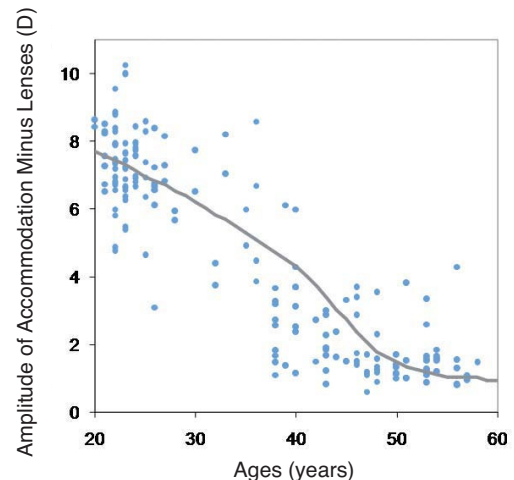


FIGURE 3 Subjective amplitude of accommodation values obtained using the Badal optometer as a function of age. The solid line represents the adapted mean amplitude of accommodation obtained by Duane.²³

Before collecting the data, we ran at least three trials, so that the subject could understand the task well and with the aim of getting an idea about the range of accommodation. This stimulus accommodation range was calculated for each subject according to Hofstetter formula²⁰ and was increased by at least 2.5 D to guarantee that the stimulus would cover the subject's full range of accommodation. For subjects younger than 35 years old, the range used was 10 D. In the few cases where the accommodation response measured by the aberrometer did not show a maximum value (indicating that the target failed to get closer than the near point), the stimulus accommodation range was increased by 2 D, and the set of accommodation measurements was repeated.

At the end of each measurement of the set of accommodation wavefronts, the aberrometer displayed the accommodation response computed using the same procedure that had been previously employed to obtain the initial refraction. Among the three repeated set of measurements, we selected again the one with the largest AA. In general, the differences between all of them were usually smaller than 1 D, although it depends on the particular subject's ability to accommodate (see López-Gil et al.¹⁷, for details on the repeatability of the measurement). The set of wavefronts corresponding to the accommodated eye are named $W_i(T_i)$, with $i=1$ to $i \leq 21$.

The Zernike expansion depended on the size of the subject's pupil. For most of subjects it was made up to the 8th order, with the minimum being 5th order (corresponding to small pupils under accommodation of some subjects). To mimic as much as possible natural viewing conditions, no mydriatic drugs were used and wavefronts were obtained under natural pupil size, so the study has taken into account natural accommodative miosis. For most of the subjects, when the target was closer than their near point, a pupil diameter increase was observed due to a relaxation in their accommodation. Prior to the accommodation measurements, the subjects were initially instructed to keep the target as clear as possible all the time as well as to blink frequently

(the aberrometer software automatically eliminates Shack-Hartmann images affected by blinks). The visual target was a figure of a balloon at the end of a road. The stimulus had a luminance of 50 cd/m², was polychromatic and contained multiple spatial frequencies.

Wavefront Determination of the Refractive State

For each optical quality metric, M_i , we computed the refractive error of the relaxed eye ($R_{0j}=M_i[W_0(T_0)]$), and the refractive state of the accommodated eye for each value of stimulus vergence, T_i , ($R_{ij}=M_i[W_i(T_i)]$). The computation finds the lens power that, when added to the eye's wavefront aberration, maximizes the value of the metric. Then, taking into account that the response of the unaccommodated eye is zero, the accommodation response for a certain normalized stimulus accommodation, T_i-R_{0j} , corresponds to $R_{ij}-R_{0j}$. AA was then estimated for this same metric as the maximum range of accommodation response, that is, the maximum value of the eye's refractive state minus the minimum value of the refractive state.

All subjective measurements were carried out by the same researcher, who was different from the researcher involved in the objective measurements. Each researcher was aware of the results obtained by his colleague. For each subject, the experiment took about 2 hours including a break in between of about 20'. The whole experiment took about two years and a half.

RESULTS

Figure 2 compares the subjective AA measured with both methods. Least-square fit line shows a slope very close to the expected one due to the fact that both methods assess the same behavior. Although, theoretically, the Badal optometer should be more precise accurate, the SD error bars corresponding to that method (horizontal bars) are usually larger than the bars corresponding to the minus-lens method (vertical bars) probably due to the fact that a 0.25 D precision is acceptable enough, and that usually two out of three

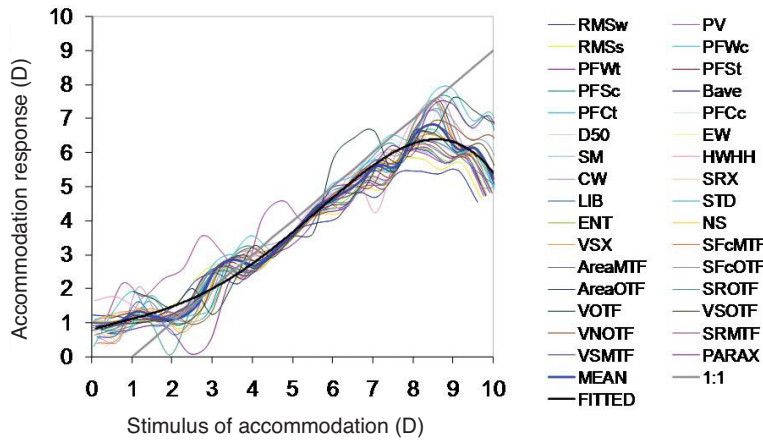


FIGURE 4 Example of the accommodation-response curves for all the metrics analyzed, for one particular subject (23 years old). A polynomial curve has been fitted ($y = 0.0012x^4 - 0.0459x^3 + 0.4564x^2 - 0.7571x + 1.2555$, $r^2 = 0.9715$) to the mean average value of the accommodation response of the 32 metrics (blue curve). The 1:1 line intersects the X-axis at the minimum value of the fitted curve (1 D).

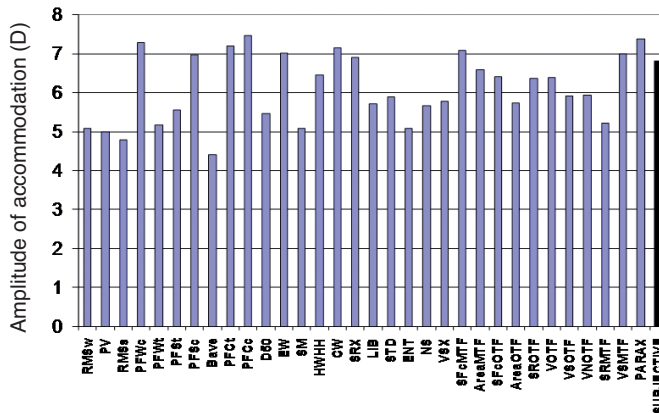


FIGURE 5 Amplitude of accommodation obtained following the different 32 objective metrics, as well as the subjective one detailed in the text.

measurements corresponding to the far or to the near point gave the same value as the power of the trial lens.

Figure 3 shows the effect of age on the subjective AA values obtained using the Badal optometer. For comparison purposes, we also show the mean AA obtained by Duane.²³ Duane's results have been slightly modified because his data were referred to the spectacle plane (placed 12 mm in front of the eye) and reduced by 20% due to the overestimated values yielded by the push-up method relative to those yielded by the minus-lenses method.²⁴ Figures 2 and 3 indicate that the subjective data collected by two independent methods are internally consistent and in broad agreement with published norms for the human eye.

Figure 4 shows an example of the accommodation response curves for each of the 32 metrics, for a 23-year-old subject. Note that although target vergence is independent of the metric of choice, the stimulus to accommodation indicated on the abscissa depends on the metric used because it depends on the vergence of R_{0j} of the far-point, which varies with the metric. The various curves do not converge at the origin because the refraction value (R_{0j}) was obtained in a separate, preliminary experiment. Thus, the refractive state of the eye during the accommodation experiment could be slightly different to the value obtained with the fogging technique (see the Methods section). For this particular

subject, response was positive for 0 D of accommodation stimulus according to all the metrics, indicating that the eye was probably more relaxed during the refraction measurements or that, possibly, a small difference in pupil diameter affected the refraction. Nevertheless, our measure of AA was not affected by these non-zero y-intercepts. The form of the stimulus-response curve was similar for most metrics, which is to be expected since they are highly correlated measures of image quality.²² Some of the jumps (such as those observed for 4 or for 7.5 D of stimulus vergence) are probably due to the fact that the target moves by steps.

The AA derived from figure 4 (i.e., for that particular 23-year-old subject) varied significantly between metrics, as shown in figure 5. Some metrics, such as PV or VOTE, have larger variations during the accommodation process. The metric that resulted in the maximum AA was PFCC, with a value of 7.5 D, while Bave metric yielded the minimum value: 4.4 D. That is, a difference of 3 D was found for this subject between the AA obtained with these two metrics. The average value of the AA across all the metrics was 6.1 D, with a standard deviation of 0.9 D. For this subject, the subjective measurement of the AA (shown by the last bar of figure 5) gave a value of 6.8 D with a standard deviation of 0.3 D. For this particular subject, SRX was the metric that most accurately predicted the subjective AA, with a value of

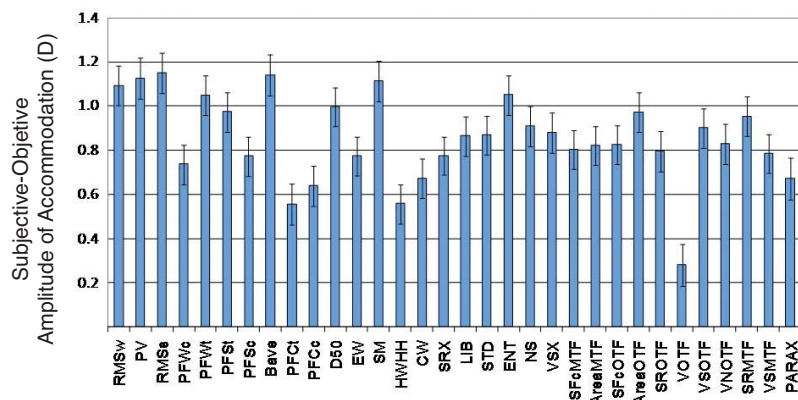


FIGURE 6
Average data for all the subjects of the difference between the amplitude of accommodation obtained with the Badal optometer and the one obtained objectively after applying the different metrics. Error bars represent \pm SEM (standard error of the mean).

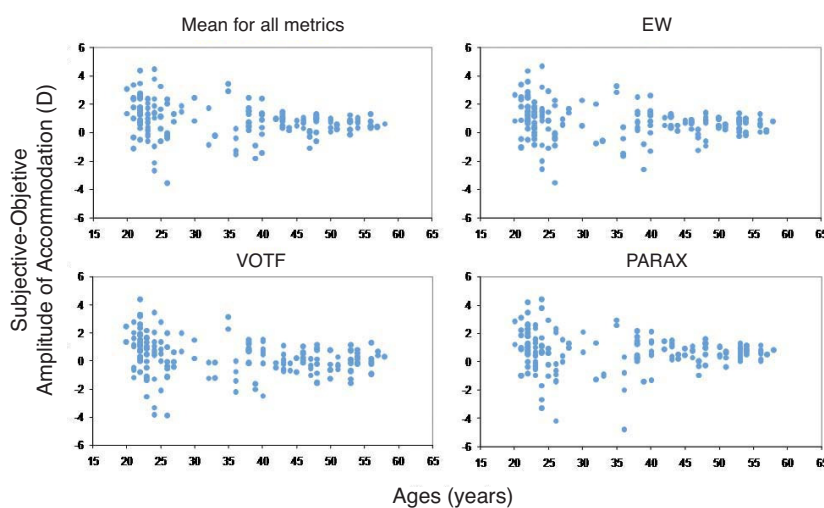


FIGURE 7
Difference in AA between subjective and objective methods as a function of age, computed using two metrics that gave good results when they were used by Thibos and coworkers²² to predict the refraction state of the relaxed eye. VOTF is also included, since it gave the best results in our study, as well as the RMS, which is perhaps the most widely used metric.²²

6.9 D. Most of the metrics (23 out of 32) yielded AA values than that were lower than the one obtained with the subjective measurement.

Figure 6 shows the average across subjects of the difference between the subjective AA (obtained with the Badal optometer) and the objective amplitude of accommodation computed using the different metrics. All metrics revealed a similar trend: the subjective AA is higher than the objective AA. The smallest discrepancy (0.19 D) was for the VOTF. The largest discrepancy (1.06 D) was for the RMSs. Error bars in the figure indicate the precision of each metric’s prediction of the subjective AA. The minimum SD (1.48 D) was achieved by the EW and the maximum SD (1.82 D) was for the paraxial (Seidel) metric PARAX.

Figure 7 shows the difference between subjective and objective measures of AA as a function of age obtained for two metrics that gave good results when they were used by Thibos and coworkers²² to predict the refractive state of the relaxed eye. The figure also includes the VOTF, which gave the highest accuracy (smallest discrepancy) in our study, as well as the RMS (i.e. Zernike refraction) which is perhaps the most widely used metric nowadays. VOTF clearly showed a best average prediction of the subjective AA, compared with the rest.

Figure 8 shows the matrix values corresponding to Pearson’s correlation between subjective-minus-objective

results obtained using different metrics. A maximum theoretical correlation corresponds to 1. From figure 8 it can be seen that the metric VOTF shows the lowest Pearson correlation (values between 0.82 and 0.90) as compared with the rest of the metrics. Metric PFCt and HWHH also showed a Pearson correlation that was lower than that yielded by the other metrics under analysis.

DISCUSSION

Our main finding (Figure 6) is that objective measurement of the accommodation amplitude determined for any of the 32 metrics of optical quality underestimates the subjective AA. The amount of underestimation depends on the maximum AA, which is usually about 1.5-2 D for subjects that are between 20 and 25 years old, and about 0.5-1 D for older eyes (see Figure 7). One potential explanation for this discrepancy between subjective and objective results is that the measurements are referenced to different planes. Wavefront measurements are referenced to the entrance pupil, whereas subjective measurements are calculated relative to the anterior corneal plane. Wavefront propagation between these two planes might account for the discrepancy. However, we think that this is rather unlikely for two reasons. First, AA is a differential measurement and, therefore, a small offset in the reference plane should have the same

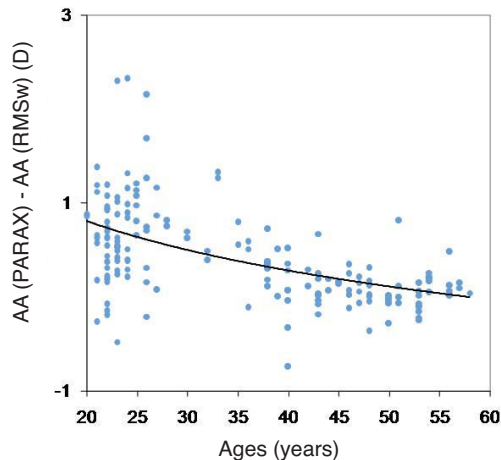


FIGURE 9
Difference between the AA obtained using PARAX and that obtained using RMSw as metric, plotted as a function of age. Fitting curve: $y = -0.7596 \ln(x) + 3.0878$; $r^2 = 0.224$.

group of 15 young subjects. Equations 1 and 2 show how the AA is calculated for the RMSw and the PARAX metrics, respectively:

$$AA = \frac{4\sqrt{3}}{r^2} (z_2^0 - \underline{z}_2^0) \quad (1)$$

$$AA = \frac{4\sqrt{3}}{r^2} (z_2^0 - \underline{z}_2^0) - \frac{12\sqrt{5}}{r^2} (z_4^0 - \underline{z}_4^0) + \frac{24\sqrt{7}}{r^2} (z_6^0 - \underline{z}_6^0) \quad (2)$$

where z_i^0 , $i = 2, 4$ or 6 , corresponds to the unaccommodated eye, and \underline{z}_i^0 , $i = 2, 4$ or 6 , corresponds to the fully accommodated eye. Since the first term in Eq. 2 is identical to the only term in Eq. 1, the difference in AA between these two metrics is due entirely to spherical aberration. Thus, we should expect AA to be higher for PARAX than for RMSw. That expectation was confirmed by López-Gil et al.³³ who found an average difference of 0.75D.

The present results shown in *figure 6* add further evidence to the fact that, if it can be assumed that Eq. 2 represents a good metrics to predict the refraction, as have been showed before,²² spherical aberration does extend the eye's AA. For our study population the PARAX metric yielded a larger AA (0.42 D more, on average) than the RMSw metric did. As indicated by Eq. 1,2 the value of this difference will depend on the amount of spherical aberration, which, in turn, depends on the maximum AA. Thus, we would expect the difference in AA (between the value determined by PARAX and the value obtained by means of RMSw) to be greater for younger subjects. This prediction is confirmed in *figure 9*. The data have been fitted using a logarithmic function which approaches a zero value for the older subjects:

$$y = -0.7596 \ln(\text{age}) + 3.0878$$

Although the regression coefficient of the fit was not high ($R^2 = 0.22$), it can be seen that for subjects under 25

years old, an average increase of 0.75 D in the AA was obtained when the effect of spherical aberration was included in the calculation. *Figure 9* shows that for most of our subjects the use of PARAX metric gave a larger AA than RMSw, this difference being in some cases as high as 2.3 D. This can be explained by taking a look at Eq. 1, 2 and by taking into account the fact that during accommodation, Z_4^0 decreases and eventually changes sign, while Z_6^0 usually increases.³³

It is worth stressing that these two metrics, RMSw and PARAX, are the only metrics used in this article that gave, in a very direct way (Eq. 1 and 2), the accommodation state of the eye from the Zernike coefficients and the associated pupil radius. Both are metrics applied at the pupil plane directly to wavefront error functions and, therefore, are indirect measures of the retinal image quality.

CONCLUSIONS

The main conclusion of our study is that objective measurements of the AA show lower values than subjective estimations of the AA, with a discrepancy that ranges from 0.2 to 1.1 D, depending on the metric used for wavefront refraction. This result can be interpreted as an underestimation of the objective data with respect to the subjective one, or as an overestimation of the subjective values with respect to the objective ones. It would depend on whether in the definition of amplitude of accommodation we only include the change of dioptric power or we include as well the pseudo-accommodation procured by the DoF.

There is a significant individual variation in this result, with an average standard deviation across metrics of 1.2 D and a standard error of the mean of 0.1 D, which decreases with age. Despite intersubject variability, the decrease of the fourth-order spherical aberration during accommodation increases the objective AA in the young eye. This increase could even exceed two diopters.

REFERENCES

1. Young T. On the mechanism of the eye. *Philos Trans R Soc Lond.* 1801;91:23-88.
2. Atchison DA, Capper EJ, McCabe KL. Critical subjective measurement of amplitude of accommodation. *Optom Vis Sci.* 1994;71:699-706.
3. Bennett AG, Rabetts RB. *Clinical Visual Optics.* 2nd Edition. London: Ed. Butterworth-Heinemann, 1995.
4. Wold JE, Hu A, Chen S, Glasser A. Subjective and objective measurement of human accommodative amplitude. *J Cataract Refract Surg.* 2003;29:1878-1888.
5. Ostrin LA, Glasser A. Accommodation measurements in a presbyopic and presbyopic population. *J Cataract Refract Surg.* 2004;30:1435-1444.
6. Aggarwala KR, Nowbotsing S, Kruger PB. Accommodation to monochromatic and white-light targets. *Invest Ophthalmol Vis Sci.* 1995; 36:2695-2705.
7. Winn B, Pugh JR, Gilmartin B, Owens H. The effect of pupil size on static and dynamic measurements of accommodation using an infra-red optometer. *Ophthalmic Physiol Opt.* 1989;9:277-283.
8. Wolffsohn JS, Hunt OA, B Gilmartin. Continuous measurement of accommodation in human factor applications. *Ophthalmic Physiol Opt.* 2002;22:380-384.
9. Gwiazda J, Thorn F, Held R. Accommodation, accommodative convergence, and response AC/A ratios before and at the onset of myopia in children. *Optom Vision Sci.* 2005;82:273-278.
10. Mordi JA, Ciuffreda KJ. Dynamic aspects of accommodation: age and presbyopia. *Vision Res.* 2004;44:591-601.
11. Cullhane HM, Winn B. Dynamic accommodation and myopia. *Invest Ophthalmol Vision Sci.* 1999;40:1968-1974.

12. Ciuffreda KJ, Rumpf D. Contrast and accommodation in amblyopia. *Vision Res.* 1985;25:1445-1457.
13. He JC, Burns SA, Marcos S. Monochromatic aberrations in the accommodated human eye. *Vision Res.* 2000;40:41-48.
14. Ninomiya S, Fujikado T, Kuroda T, et al. Changes of ocular aberration with accommodation. *Am J Ophthalmol.* 2002;134:924-926.
15. Cheng H, Barnett JK, Vilupuru AS, et al. A population study on changes in wave aberrations with accommodation. *J Vis.* 2004;4:272-280.
16. López-Gil N, Rucker FJ, Stark LR, et al. Effect of coma and trefoil on dynamic accommodation. *Vision Res.* 2007;47:755-765.
17. López-Gil N, Fernández-Sánchez V, Legras R, Montés-Micó R, Lara F, Nguyen-Khoa JL. Accommodation-related changes in monochromatic aberrations of the human eye as a function of age. *Invest Ophthalmol Vis Sci.* 2008;49:1736-1743.
18. Win-Hall DM, Glasser A. Objective accommodation measurements in presbyopic eyes using an autorefractor and an aberrometer. *J Cataract Refract Surg.* 2008;34:774-784.
19. Larry Thibos, Nikole Himebaugh, Charles D. Coe. Wavefront refraction. Chapter 19 in *Borish's Clinical Refraction 2nd Ed.* Benjamin WJ (editor), New York: Butterworth-Heinemann –Elsevier, 2006.
20. Scheiman M, Wick B. *Clinical Management of Binocular Vision.* New York: Lippincott, 1994.
21. López-Gil N, Iglesias I, Artal P. Retinal image quality in the human eye as a function of accommodation. *Vision Res.* 1998;39:2897-2907.
22. Thibos LN, Hong X, Bradley A, Applegate RA. Accuracy and precision of objective refraction from wavefront aberrations. *J Vis.* 2004;4:329-351.
23. Duane A. Studies in monocular and binocular accommodation with their clinical applications. *Am J Ophthalmol.* 1922;5:865-877.
24. Wold JE, Hu A, Chen S, Glasser A. Subjective and objective measurement of human accommodative amplitude. *J Cataract Refract Surg.* 2003;29:1878-1888.
25. López-Gil N, Castejón-Mochón JF, Fernández-Sánchez V. Limitations of the ocular wavefront correction with contact lenses. *Vision Res.* 2009;49:1729-1737.
26. Charman WN, Tucker J. Dependence of accommodation response on the spatial frequency spectrum of the observed object. *Vision Res.* 1977;17:129-139.
27. Johnson CA. Effects of luminance and stimulus distance on accommodation and visual resolution. *J Opt Soc Am.* 1976;66:138-142.
28. Charman WN, Whitefoot H. Pupil diameter and the depth of field of the human eye as measured by laser speckle. *Optica Acta.* 1977;24:1211-1216.
29. Dalimier E, Pailos E, Rivera R, Navarro R. Experimental validation of a personalized Bayesian model of visual acuity. *J Vis.* 2009;9:1-16.
30. Cheng X, Bradley A, Thibos LN. Predicting subjective judgment of best focus with objective image quality metrics. *J Vis.* 2004;4:310-321.
31. Charman WN, Tucker J. Accommodation and color. *J Opt Soc Am.* 1978;68:459-471.
32. Buehren T, Collins MJ. Accommodation stimulus-response function and retinal image quality. *Vision Res.* 2006;46:1633-1645.
33. Lopez-Gil N, Lara F, Fernandez-Sanchez V. Effect Of Pupil Miosis And Spherical Aberration On The Accommodation Response *Invest Ophthalmol Vis Sci* 2006;47: E-Abstract 5844.

APPENDIX A

Acronym	Metric	Expression
RMSw	RMS of the wavefront error	$\sqrt{\frac{1}{A} \int_{pupil} (w - \bar{w})^2 dx dy}, M = \frac{-4\sqrt{3}z_2^0}{r^2}$
PV	Peak-to-valley difference of the wavefront	$\max(w) - \min(w)$
RMSs	RMS of the wavefront slope	$\sqrt{\frac{1}{A} \int_{pupil} [(w_x - \bar{w}_x)^2 + (w_y - \bar{w}_y)^2] dx dy}$
PFWc	Pupil fraction satisfying RMS criterion for wavefront phase	$\left(\frac{\text{critical circ. diam.}}{\text{pupil diameter}}\right)^2, RMSw < \text{criterion}$
PFWt	Pupil fraction satisfying PV criterion for wavefront phase	$\frac{\text{Area good subaperture}}{\text{pupil area}}, PVw < \text{criterion}$
PFSs	Pupil fraction satisfying PV criterion for wavefront slope	$\frac{\text{Area good subaperture}}{\text{pupil area}}, PVs < \text{criterion}$
PFSc	Pupil fraction satisfying RMS criterion for wavefront slope	$\left(\frac{\text{critical circular diam.}}{\text{critical diam.}}\right)^2, RMSs < \text{criterion}$
Bave	Average blur strength	$\frac{1}{\text{pupil area}} \int_{pupil} \sqrt{M^2(x, y) + J^2(x, y)} dx dy,$ $M = \frac{k_1 + k_2}{2}, J = \frac{k_1 - k_2}{2}, k_1 \text{ and } k_2 = \text{principal curvatures}$
PFCt	Pupil fraction satisfying average blur strength criterion, wave curvature	$\frac{\text{Area good subaperture}}{\text{pupil area}}, B_{PV} < \text{criterion}$
PFCc	Pupil fraction satisfying maximum blur strength criterion for wave curvature	$\left(\frac{\text{critical circular diam.}}{\text{critical diam.}}\right)^2, B_{ave} < \text{criterion}$
D50	Diameter of the PSF with 50% of the energy	$2\pi r$ $r, \iint_0^{2\pi} PSF_N(r, \vartheta) = 0.5$
EW	Equivalent width of the centered PSF	$\sqrt{\frac{4 \int_{pupil} PSF(x, y) dx dy}{\pi PSF(x_0, y_0)}}$
SM	Square root of second moment of light distribution	$\sqrt{\frac{\int_{pupil} (x^2 + y^2) PSF(x, y) dx dy}{\int_{pupil} PSF(x, y) dx dy}}$
HWHH	Half width at half height of the PSF	$\sqrt{\frac{\int_{pupil} C(x, y) dx dy}{\pi}}$ $\text{with } C = 1 \text{ if } PSF > \max\left(\frac{PSF}{2}\right), \text{ otherwise } C = 0 \quad (.../...)$

APPENDIX A (continued)

Acronym	Metric	Expression
CW	Correlation width of light distribution	$\frac{\int_{-\infty}^{\infty} \int_{-\infty}^{\infty} Q(x, y) dx dy}{\pi}$ <p>with $Q = 1$ if $PSF \otimes PSF > (PSF \otimes PSF) / 2$, otherwise $Q = 0$</p>
SRX	Strehl ratio computed in spatial domain	$\frac{\max(PSF)}{\max(PSF_{Dif.Lim.})}$
LIB	Light-in-the-bucket (core of diffraction limited PSF)	$\int_{Dif.Lim.core} PSF_N(x, y) dx dy$
STD	Standard deviation of intensity in the PSF	$\sqrt{\frac{\int_{pupil} (PSF - \overline{PSF})^2 dx dy}{\int_{pupil} (PSF_{Dif.Lim.} - \overline{PSF_{Dif.Lim.}})^2 dx dy}}$
ENT	Entropy of the PSF	$\int_{PSF} PSF \ln(PSF) dx dy$
NS	Neural sharpness	$\frac{\int_{PSF} PSF(x, y) g(x, y) dx dy}{\int_{PSF} PSF_{Dif.Lim.}(x, y) g(x, y) dx dy}$ <p>$g(x, y) = \text{neural weighting function}$</p>
VSX	Visual Strehl ratio in the spatial domain	$\frac{\int_{PSF} PSF(x, y) N(x, y) dx dy}{\int_{PSF} PSF_{Dif.Lim.}(x, y) N(x, y) dx dy}$ <p>$N(x, y) = \text{neural weighting function}$</p>
SFcMTF	Spatial frequency cutoff of radial MTF	$\max(SF) \text{ for which } rMTF > \text{neural threshold}$
AreaMTF	Area of visibility under radial average MTF (rMTF)	$\frac{\int_0^{cutoff} MTF(f) df - \int_0^{cutoff} T_N(f) df}{\int_0^{cutoff} MTF_{Dif.Lim.}(f) df - \int_0^{cutoff} T_N(f) df}$ <p>$T_N = \text{neural contrast threshold function}$</p>
SFcOTF	Spatial frequency cutoff of radial OTF	$\min(SF) \text{ for which } rOTF < \text{neural threshold}$

(.../...)

APPENDIX A

Acronym	Metric	Expression
AreaOTF	Area of visibility under radial average OTF (rOTF)	$\frac{\int_0^{cutoff} rOTF(f)df - \int_0^{cutoff} T_N(f)df}{\int_0^{cutoff} rOTF_{Dif.Lim.}(f)df - \int_0^{cutoff} T_N(f)df}$ <p>$T_N = \text{neural contrast threshold function}$</p>
SROTF	Strehl ratio computed from OTF in frequency domain	$\frac{\int_{-\infty}^{\infty} \int_{-\infty}^{\infty} OTF df_x df_y}{\int_{-\infty}^{\infty} \int_{-\infty}^{\infty} OTF_{Dif.Lim.} df_x df_y}$
VOTF	Normalized volume under the OTF	$\frac{\int_{-\infty}^{\infty} \int_{-\infty}^{\infty} OTF df_x df_y}{\int_{-\infty}^{\infty} \int_{-\infty}^{\infty} MTF df_x df_y}$
VSOTF	Visual Strehl ratio computed from OTF in frequency domain	$\frac{\int_{-\infty}^{\infty} \int_{-\infty}^{\infty} CSF_N OTF df_x df_y}{\int_{-\infty}^{\infty} \int_{-\infty}^{\infty} CSF_N OTF_{Dif.Lim.} df_x df_y}$
VNOTF	Normalized volume under the neurally-weighted OTF	$\frac{\int_{-\infty}^{\infty} \int_{-\infty}^{\infty} CSF_N OTF df_x df_y}{\int_{-\infty}^{\infty} \int_{-\infty}^{\infty} CSF_N MTF df_x df_y}$
SRMTF	Strehl ratio computed from MTF in frequency domain	$\frac{\int_{-\infty}^{\infty} \int_{-\infty}^{\infty} MTF df_x df_y}{\int_{-\infty}^{\infty} \int_{-\infty}^{\infty} MTF_{Dif.Lim.} df_x df_y}$
VSMTF	Visual Strehl ratio computed from MTF in frequency domain	$\frac{\int_{-\infty}^{\infty} \int_{-\infty}^{\infty} CSF MTF df_x df_y}{\int_{-\infty}^{\infty} \int_{-\infty}^{\infty} CSF_{Dif.Lim.} MTF_{Dif.Lim.} df_x df_y}$
PARAX	Paraxial curvature matching	$M = \frac{-4\sqrt{3}z_2^0 + 12\sqrt{5}z_4^0 - 24\sqrt{7}z_6^0}{r^2}$